Steep Slope DEM Model Construction based on the Unmanned Aerial Vehicle (UAV) Images

(Pembinaan Model DEM Cerun Curam berdasarkan Imej Kenderaan Udara Awasan Automatik (UAV))

WENFEI XI* & DONGSHENG LI

ABSTRACT

The DEM construction of high and steep slope has great importance to slope disaster monitoring. The conventional method used to construct high and steep slope DEM model requires larger field surveying workload. First of all, the high and steep slope image was obtained through unmanned aerial vehicle (UAV) platform; Then the SIFT algorithm is used to extract the feature points which are going to be matched accurately by using RANSAC algorithm. Finally, stereo pair splicing method is used to generate orthogonal images and construct DEM model. After comparing the DEM model with actual slope measurement result collected by total station finding, it is shown that elevation error between the DEM model constructed by unmanned aerial vehicle (UAV) and actual measurement is minimal and its efficiency is proven.

Keywords: DEM model; high and steep slope; orthogonal image; SIFT algorithm; unmanned aerial vehicle (UAV)

ABSTRAK

Pembinaan DEM di cerun tinggi dan curam adalah penting kepada pemantauan bencana cerun. Kaedah konvensional yang digunakan untuk membina model DEM cerun tinggi dan curam memerlukan beban kerja pengukuran lapangan lebih besar. Pertama, imej cerun yang tinggi dan curam diambil melalui platform kenderaan udara awasan automatik (UAV); kemudian, algoritma SIFT digunakan untuk mendapatkan ciri butiran yang akan dipadankan dengan tepat menggunakan algoritma RANSAC. Akhir sekali, kaedah penyambatan pasangan stereo digunakan untuk menjana imej ortogonal dan membina model DEM. Selepas membandingkan keputusan model DEM dengan pengukuran cerun sebenar yang dikumpul melalui jumlah stesen, ditunjukkan bahawa ralat penaikan antara model DEM yang dibina oleh kenderaan udara awasan automatik (UAV) dan pengukuran sebenar adalah minimum dan kecekapannya telah dibuktikan.

Kata kunci: Algoritma SIFT; cerun tinggi dan curam; kenderaan udara awasan automatik (UAV); imej ortogon; model DEM

INTRODUCTION

Due to lower flying height, small clouds block effects, to some extent, UAV photogrammetry can supplement aerial survey. With the advantages of flexibility, convenience, speediness and efficiency, unmanned aerial vehicle (UAV) can greatly improve the efficiency of data acquisition and reduce the dependence on the photography environment. As a result, it can be used to obtain high resolution image quickly and accurately (Abd Rahman et al. 2016; Colomina & Molina 2014; Gerke & Przybilla 2016; Harwin & Lucieer 2012). UAV images can be geometrically reconstructed to obtain digital surface models and point cloud data (Nex & Remondino 2014), which can be widely used in archaeology, vegetation monitoring, traffic monitoring and disaster management (Berni et al. 2009; Eisenbeiss & Sauerbier 2011; Fernández-Hernandez et al. 2015; Puri et al. 2007; Zhang & Kovacs 2012). Chai et al. (2015) carried out the landscape DEM construction by the mean of unmanned aerial vehicle (UAV); Zhang et al. (2014) adopted unmanned aerial vehicle (UAV) to build

3D terrain, which can meet the requirement of the 1:1000 three dimensional terrains in flat areas.

In the construction of UAV image DEM model, the quality of image splicing directly affects the precision of the model. There are some obstacles to be tackled in the rectification process, such as rotation and scale transformation, geometric distortion and rotation angle. The common feature points extraction algorithms mainly include: Harris corner algorithm (Harris & Stephens 1988; Zhang et al. 2014), SIFT (scale invariant feature transform) algorithm (Lowe 1999) and SURF (speeded up robust features) algorithm (Bay et al. 2008). The feature point is used to match, calculate the matching model parameters and realize the image rectification. The feature point matching algorithm has low computational complexity, high rectification accuracy and good robustness to noise effects and image distortion (Li 2008). Some mathematical formulas used in this article can refer to (Gao & Guo 2016; Gao & Wang 2016; Gao et al. 2016; Zhao & Chen 2017).

This paper takes a high-steep slope in Kunming as the research object and uses unmanned aerial vehicle (UAV) photography technology to construct the DEM model which is compared with the total station sampling data later. Mainly used SIFT algorithm in the test is described as below.

SIFT ALGORITHM PRINCIPLE

THE ESTABLISHMENT OF GAUSSIAN DIFFERENTIAL PYRAMID

The SIFT algorithm, proposed by Lowe (1999), is a feature-based matching algorithm based on scale space, mainly using Gaussian differential pyramid model (Forstner & Gulch 1987; Roslee et al. 2017). The Gaussian pyramid is essentially a multi-scale representation of the signal, Gaussian blurring the same signal or picture many times and down-sampling to produce multiple sets of signals or pictures at different scales for subsequent processing. On the basis of a series of reasonable assumptions, Koenderink and Lindeberg proved that the Gaussian function probably is the only spatial kernel scale to realize image scale conversion. One tile of image spatial scale can be defined as:

$$L(x,y,s) = G(x,y,s) * I(x,y) \quad (1)$$

where * represents the sum of convolution operation, (x, y) denotes the space coordinates of pixel; s is scale coordinates of pixel; and $G(x, y, s)$ is scale variable Gaussian kernel function, which is defined as:

$$G(x,y,s) = \frac{1}{2ps^2} e^{-(x^2+y^2)/2s^2} \quad (2)$$

Lowe (1999) raised that it uses Gaussian difference operator to establish image Gaussian difference scale space. It is able to obtain Gaussian difference images $D(x, y, s)$ with different scales by using the Gaussian difference kernels and image convolution on different scales. All Gaussian difference images together make up the Gaussian difference pyramid of the image.

where

$$D(x,y,s) = (G(x,y,ks) - G(x,y,s)) * I(x,y) = L(x,y,ks) - L(x,y,s) \cdot \quad (3)$$

Construction process of image Gaussian difference pyramid is shown in the left part of Figure 1. In the group, the images from the upper layer are convoluted with the Gaussian functions of different scales to obtain the spatial images in which the constant scale factor is increased k times. In other words, the scale of first layer is s, the scale of second layer is ks, and the next layer follows this rule. The image of the first layer of each group is obtained from the first layer sample of the previous set of images. The size of the image after sampling is 1/4 of the size of the images of the previous group, but scale size is twice of the original one. In this way, the Gaussian difference pyramid is constructed.

The right part of Figure 1 describes the process how to construct Gaussian difference pyramid. In the group, Gaussian difference image is obtained after the subtraction between adjacent images. Then, after repeating the previous operations on the full set of images, we get the Gaussian difference pyramid.

GENERATION OF FEATURE POINT DESCRIPTOR

After the key point SIFT feature area is generated, firstly the axis direction is rotated to the main direction of the key points, which ensures the rotation invariance. Then we select the neighborhood window with the key as the center, as shown in the left part of Figure 2.

The central pixel is the key point to be described. The surrounding little grids represent the pixels of the neighborhood key points; the length of the arrow represents the gradient value of the pixel and the direction of the arrow represents the gradient direction of the pixel. The circles in the figure represent the range of Gaussian weighting of pixel values. As shown in right part of Figure 2: In every sub block, if we calculate the gradient direction histogram in eight directions, we can get a seed point. When all the seed points are obtained, we get a descriptor.

In order to verify the stability of the SIFT algorithm, different terrain features are chosen to be extracted and we use SIFT operator to extracts feature points of buildings (638 × 535), shrub (858 × 583), respectively. As shown in Figure 3, the red points are the feature points, which mean that feature points distributed evenly.
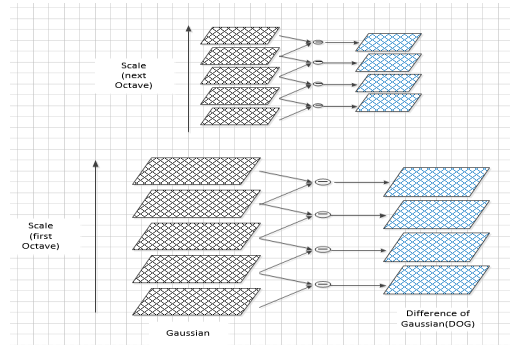

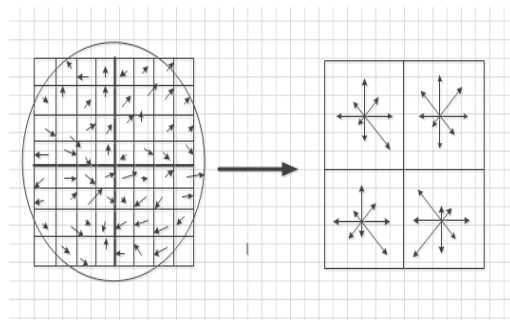FIGURE 1. The generation of Gaussian difference pyramid

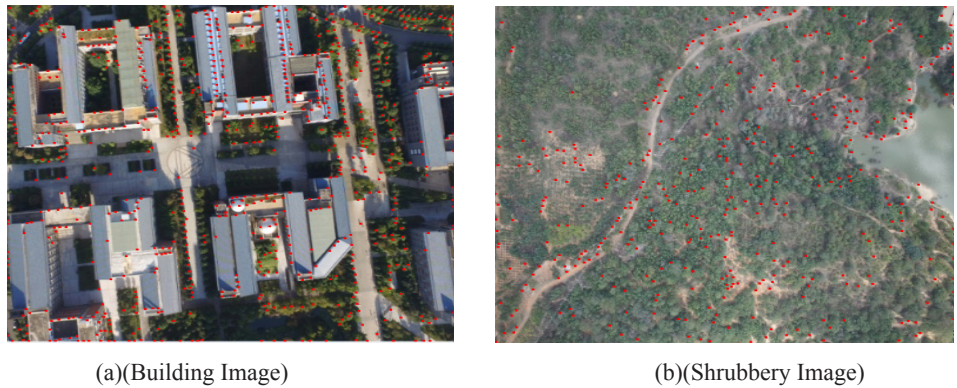FIGURE 2. Feature vector generated by critical point neighborhood gradient information

<div style="text-align:center">(a)(Building Image)   (b)(Shrubbery Image)</div>

FIGURE 3. SIFT operator feature extraction

<div style="text-align:center">(a) (UAV)   (b) (UAV)</div>

FIGURE 4. Six rotor unmanned aerial vehicle

THE EXPERIMENTAL CASE

This paper uses the six rotor unmanned aerial vehicle (UAV) which is equipped with GPS/GLONASS double mode, 12.4 million pixels camera (as shown in Figure 4) to collect data. The design of this experiment is described as follows:

First: Unmanned aerial vehicle (UAV) is used to obtain the original slope image data in a light even condition. Second: The quality of the acquired image data must be checked. The software is used to check whether the image meets the quality requirements of modeling. If not, the UAV must fly again to collect enough data. Third: The SIFT algorithm is used to splice image data and precise matching algorithms are used to eliminate matching error. Fourth: Slope DEM model is constructed and Fifth: Field data are gathered and data comparison is compared

Sample images are collected by unmanned aerial vehicle (UAV) and we choose one of them which is shown in (Figure 5). The flight height of unmanned aerial vehicle (UAV) is 150 m. The ground resolution is 4 cm. The photo course overlap degree is 80%. The side overlap degree is 70% and the course lines are 4 (Figure 6). The quality of the obtained image data is checked and aligned.

FIGURE 5. Slope image

FIGURE 6. Course lines chart

UAV IMAGE DATA PROCESSING

SIFT splice algorithm is used to conduct image stitching. Before the image stitching, feature points are extracted and the extraction results are shown in Figure 7. It is seen that the feature points which are described as red points, distributed evenly near the road and slope.

The result of feature points extracted coarse matching can be seen from Figure 8. After a coarse matching, it appeared cross connections in figure. There are rectification errors in the matching process, which needs to be eliminated. This study adopts the RANSAC (Random Sample Consensus) algorithm to remove coarse error, after which the corresponding points are matched. The result is shown in Figure 9.

SIFT splice algorithm is used to spice the images and the result of overlapping images is shown in Figure 10. The spliced orthogonal image and the constructed DEM model are shown in Figures 11-12 separately.

(a) (UAV image)
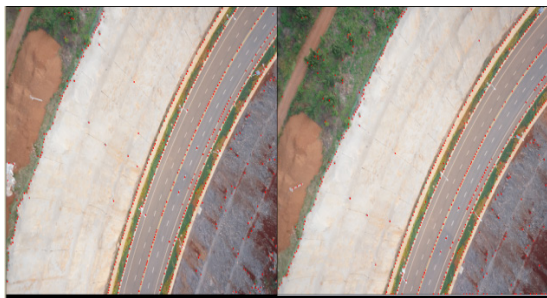
(b) (Feature points)

FIGURE 7. UAV image feature extraction

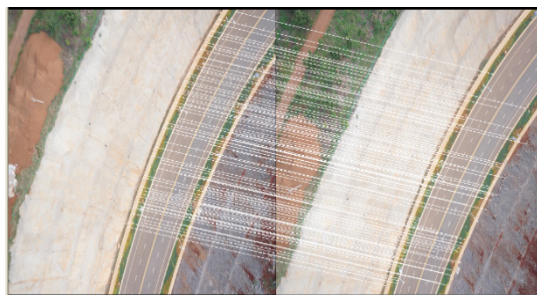FIGURE 8. Coarse matching of image feature
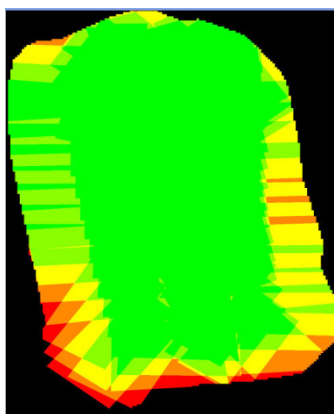

FIGURE 9. Image feature matching
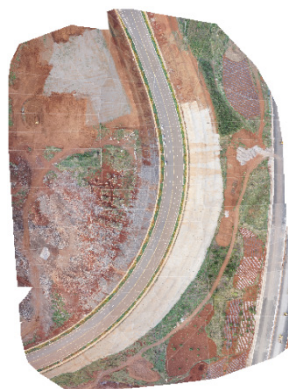

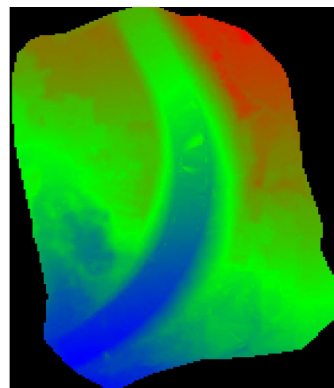FIGURE 10. Images overlap

FIGURE 11. Orthogonal image

FIGURE 12. UAV DEM model

The total station is used to measure the terrain of 1: 1000 for high and steep slopes. The actual measured data are used to construct the contour which is shown in Figure 13. The DEM model for the measured data is shown in Figure 14.
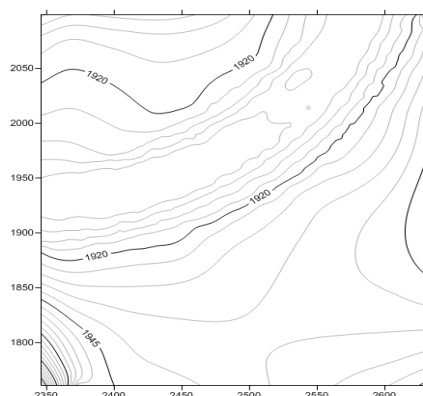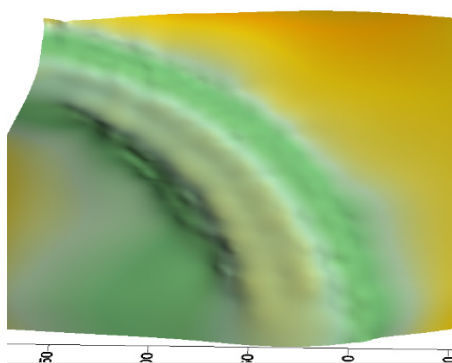

FIGURE 13. Contour

FIGURE 14. Experimental area DEM model

We compare the elevation point data extracted from model 12 and 14. Then we find that the maximum elevation error is 0.5 min plain area and the maximum elevation error is 1.2 min the slope area. In addition, viewed from the look of the constructed model, the two models are relatively similar.

CONCLUSION

Based on the unmanned aerial vehicle (UAV) images, the paper constructed steep slope DEM model. In details, the DEM model is constructed using the feature data to conduct the coarse matching and accurate matching and the matching results of the model is verified by adopting field measurements method. The results showed that the model constructed using unmanned aerial vehicle (UAV) images can meet the demand of 1:2000 terrain. As a result, the use of UAV to construct model can reduce the workload of the field, improve working efficiency, and it can be used for the model constructions of environmental and landscape.

REFERENCES

Abd Rahman, N.H., Lee, M.H., Suhartono & Latif, M.T. 2016. Evaluation performance of time series approach for forecasting air pollution index in Johor, Malaysia. *Sains Malaysiana* 45(11): 1625-1633.

Bay, H., Ess, A., Tuytelaars, T. & Van Gool, L. 2008. Speeded-up robust features (SURF). *Computer Vision and Image Understanding* 110(3): 346-359.

Berni, J., Zarco-Tejada, P., Suárez, L., González-Dugo, V. & Fereres, E. 2009. Remote sensing of vegetation from UAV platforms using lightweight multispectral and thermal imaging sensors. *Proc. ISPRS* 38: 22-29.

Chai, Z.W., Kang, J., Wang, L., Zhao, X. & Qiao, H.L. 2015. The construction of DEM in mountain plantation landscape based on UAV images. *Remote Sensing Technology and Application* 30(3): 504-508.

Colomina, I. & Molina, P. 2014. Unmanned aerial systems for photogrammetry and remote sensing: A review. *ISPRS J. Photogramm. Remote Sens.* 92: 79-97.

Eisenbeiss, H. & Sauerbier, M. 2011. Investigation of UAV systems and flight modes for photogrammetric applications. *Photogramm. Rec*. 26: 400-421.

Fernández-Hernandez, J., González-Aguilera, D., Rodríguez-Gonzálvez, P. & Mancera-Taboada, J. 2015. Image-based modelling from unmanned aerial vehicle (UAV) photogrammetry: An effective, low-cost tool for archaeological applications. *Archaeometry* 57: 128-145.

Forstner, W. & Gulch, E. 1987. A fast operator for detection and precise location of distinct points, comers and centres of circular features. *Interlaken: Switzerland Proceeding of Intercommission Workshop on Fast Processing of Photogrammetric Data*. pp. 281-305.

Gao, W. & Guo, Y. 2016. The fifth geometric arithmetic index of bridge graph and carbon nanocones. *Journal of Difference Equations and Applications*. http://dx.doi.org/10.1080/10236198.2016.1197214.

Gao, W., Guo, Y. & Wang, K.Y. 2016. Ontology algorithm using singular value decomposition and applied in multidisciplinary, cluster computing. *The Journal of Networks Software Tools and Applications* 19(4): 2201-2210.

Gao, W. & Wang, W.F. 2016. The eccentric connectivity polynomial of two classes of nanotubes. *Chaos, Solitons and Fractals* 89: 290-294.

Gerke, M. & Przybilla, H.J. 2016. Accuracy analysis of photogrammetric UAV image blocks: Influence of onboard RTK-GNSS and cross flight patterns. *Photogramm. Fernerkund. Geoinf.* 14: 17-30.

Harris, C. & Stephens, M. 1988. A combined corner and edge detector. *Alvey Vision Conference* 15: 147-151. doi: 10.5244/C.2.23.

Harwin, S. & Lucieer, A. 2012. Assessing the accuracy of georeferenced point clouds produced via multi-view stereopsis from unmanned aerial vehicle (UAV) imagery. *Remote Sens.* 4: 1573-1599.

Li, B.L. 2008. Study of registration algorithm in image mosaic based on key points. Master Thesis of Tianjin University (Unpublished).

Lowe, D.G. 1999. Object recognition from local scale-invariant features. *The Proceedings of the Seventh IEEE International Conference on Computer Vision* 2: 1150-1157.

Nex, F. & Remondino, F. 2014. UAV for 3D mapping applications: A review. *Appl. Geomat.* 6: 1-15.

Puri, A., Valavanis, K. & Kontitsis, M. 2007. Statistical profile generation for traffic monitoring using real-time UAV based video data. In *Proceedings of the Mediterranean Conference on Control & Automation, Athens, Greece.* pp. 27-29.

Roslee, R., Simon, N., Tongku, F., Norhisham, M.N. & Taharin, M.R. 2017. Landslide susceptibility analysis (LSA) using deterministic model (infinite slope) (DESSISM) in the Kota Kinabalu area, Sabah, Malaysia. *Geological Behavior* 1(1): 06-09.

Zhang, C. & Kovacs, J.M. 2012. The application of small unmanned aerial systems for precision agriculture: A review. *Precis. Agric.* 13: 693-712.

Zhang, W.Q., Zhao, J.S. & Tang, M. 2014. Research on 3d terrain modeling by UAV image. *Engineering of Surveying and Mapping* 3(23): 36-41.

Zhao, S. & Chen, T. 2017. Design and development of national geographic condition monitoring system based on Web GIS. *Geology, Ecology, and Landscapes* 1(1): 12-18.

Wenfei Xi*
College of Tourism and Geographic Sciences
Yunnan Normal University
Kunming 650050
China

Dongsheng Li
Kunming Metallurgy College
Kunming 650033
China

*Corresponding author; email: xiwenfei911@163.com